

**Impact of dark matter direct searches and the LHC analyses on branon phenomenology**Jose A.R. Cembranos,<sup>1</sup> J. Lorenzo Díaz-Cruz,<sup>2</sup> and Lilian Prado<sup>2</sup><sup>1</sup>*Departamento de Física Teórica I, Universidad Complutense de Madrid, E-28040, Spain*<sup>2</sup>*Facultad de Ciencias Físico-Matemáticas, Benemérita Universidad Autónoma de Puebla, C. P. 72570, Puebla, Pue., Mexico*  
(Received 20 June 2011; published 20 October 2011)

Dark Matter direct detection experiments are able to exclude interesting parameter space regions of particle models which predict an important amount of thermal relics. We use recent data to constrain the branon model and to compute the region that is favored by CDMS measurements. Within this work, we also update present colliders constraints with new studies coming from the LHC. Despite the present low luminosity, it is remarkable that for heavy branons, CMS and ATLAS measurements are already more constraining than previous analyses performed with TEVATRON and LEP data.

DOI: 10.1103/PhysRevD.84.083522

PACS numbers: 95.35.+d, 11.10.Kk, 11.25.Wx

**I. INTRODUCTION**

Identifying the nature of Dark Matter (DM) is a central problem in contemporary physics. The nature of DM and how it fits into our current understanding of elementary particles is not known yet. Numerous astrophysical and cosmological data require the existence of a DM component, that accounts for about 20% of the energy content of our universe. Although there are other possibilities [1], DM is usually assumed to be in the form of stable Weakly-Interacting Massive Particles (WIMPs) that naturally freeze out with the right thermal abundance, with a mass of the order of the electroweak (EW) scale. The most studied DM candidate is the neutralino, which can be identified as the lightest supersymmetric particle in many supersymmetric models. These models own a rich phenomenology due to the large number of new particles present in the theory [2].

Besides, the existence of extra dimensions are well motivated theoretically and DM candidates arise associated to new degrees of freedom. In particular, branons have been proposed to explain the missing matter problem within the so-called brane-world scenario (BWS) [3]. In this framework, the SM fields are forced to live on a three-dimensional hypersurface called brane, while gravity propagates on the higher  $D = 4 + N$ -dimensional bulk space. The fundamental scale of gravity is not the Planck scale  $M_p$  anymore, but a new scale  $M_D$  which in this work will be considered arbitrary [3].

In this scenario, the existence of extra dimensions generates new fields on the brane, giving rise to a Kaluza-Klein (KK) tower of massive gravitons. The brane has a finite tension  $f^4$  and its fluctuations are parametrized by the so-called branon fields  $\pi^a$ . These branons are the massless Goldstone bosons arising from the spontaneous breaking of the exact symmetry existing in the case of translational invariance in the bulk space. In the general case of translational invariance explicitly broken, the branons are expected to be massive fields. When these branons are considered, the coupling of the standard model (SM)

particles to any bulk field is exponentially suppressed by a factor  $\exp[-M_{\text{KK}}^2 \Lambda^2 / 8\pi f^4]$ , where  $M_{\text{KK}}$  is the mass of the corresponding KK mode of the tower of massive gravitons and  $\Lambda$  is the cutoff of the effective theory that describes the branon phenomenology [4,5].

If the tension scale  $f$  is much smaller than the other new scales so that  $f^2 \ll \Lambda M_{\text{KK}}$ , then the KK modes decouple from the SM particles, so that at low energies the only brane-world related particles that must be taken into account are branons. In the following, we will assume this to be the case and accordingly we will deal only with SM particles and branons [3].

$\Lambda$  could represent the width of brane or any other mechanism that modified the short-distance theory to cure the ultraviolet behavior of branons. However, for our purposes,  $\Lambda$  is just a phenomenological parameter. From the point of view of the effective theory,  $\Lambda/f$  parameterizes how strongly (or weakly) coupled the quantum brane is, and therefore controls the unknown relative importance of tree-level versus loop branon effects. In [5], it was shown that the perturbative loop analysis only makes sense for approximately  $\Lambda \lesssim 4\pi^{1/2} f N^{-1/4}$ . We will work in such a limit.

These branons are expected to be nearly massless and weakly interacting at low energies. In general, translational invariance in the extra dimensions is not necessarily an exact symmetry, so that explicit symmetry breaking leads to a branon mass  $M$ . Brane fluctuations could be candidates for the cosmological DM and they could also make up the galactic halo and explain the local dynamics. Therefore, they could be detected by DM search experiments [3,6].

Several experiments have been developed to detect DM directly and indirectly. The direct DM detection experiments are designed to observe the elastic scattering of DM particles with nuclei while indirect DM searches may detect the DM annihilation productions such as protons, antiprotons, electrons, positrons, neutrinos and gamma rays. Complementary to these, collider DM searches are performed at experiments like CERN (European

Organization for Nuclear Research) LHC (Large Hadron Collider) [7,8].

The outline of the paper is as follows. We shall discuss briefly the model in Sec. II. Section III is dedicated to direct DM search experiments, reporting some DM candidate events and their relation with branons. Section IV is devoted to the analysis of branons related to collider results and new LHC constraints. Finally, Sec. V presents our conclusions.

## II. FLEXIBLE BRANE-WORLDS

The presence of branes in extra-dimensional models has been studied from many different points of view (read, for instance, [9]). We will consider a single-brane model in large extra dimensions, where the four-dimensional space-time  $M_4$  is embedded in a  $D$ -dimensional bulk space. This space is assumed to have the form  $M_D = M_4 \times B$ , where the  $B$  homogeneous space is an  $N$ -dimensional compact manifold, such that  $D = 4 + N$ . The brane lies along  $M_4$  and its contribution to the bulk gravitational field is neglected [3,6,10].

Branons couple to the conserved energy-momentum tensor of the SM evaluated in the background metric  $T_{SM}^{\mu\nu}$ . The lowest order effective Lagrangian is given by [3]:

$$\begin{aligned} \mathcal{L}_{Br} = & \frac{1}{2} g^{\mu\nu} \partial_\mu \pi^\alpha \partial_\nu \pi^\alpha - \frac{1}{2} M^2 \pi^\alpha \pi^\alpha \\ & + \frac{1}{8f^4} (4\partial_\mu \pi^\alpha \partial_\nu \pi^\alpha - M^2 \pi^\alpha \pi^\alpha g_{\mu\nu}) T_{SM}^{\mu\nu}. \end{aligned} \quad (1)$$

Branons are stable and difficult to detect because they always interact by pairs and their interactions are suppressed by the tension scale  $f$ , which implies that they can be weakly interacting. Also they are expected to be massive so that their freeze-out temperature could be relatively high and then their relic abundances could be cosmologically important. This implies that branons are natural candidates for DM in a scenario where  $f \ll M_D$  [3].

The thermal relic branon abundance is calculated in [3], where it has been considered the relativistic (hot) and nonrelativistic (cold) cases at decoupling. The allowed region for hot branons masses are much smaller than those in neutrino DM models so that they decouple much earlier than neutrinos; therefore, hot branons are disfavored. Branons could be responsible for providing the observed cosmological DM density  $\Omega_{Br} h^2 = 0.110 \pm 0.006$  [11].

## III. DM DIRECT-DETECTION EXPERIMENTS

Several DM direct-detection experiments have presented recently some results. Their reported limits are compatible with the branon scenario.

Assuming that the DM halo of the Milky Way is composed of branons, its flux on the Earth is of order  $10^5 (100 \text{ GeV}/M) \text{ cm}^{-2} \text{ s}^{-1}$ , and could be sufficiently large

to be measured in direct detection experiments such as DAMA, XENON100, CoGeNT, CDMS II, or EDELWEISS-II. These experiments measure the rate  $R$ , and energies  $E_R$  of the nuclear recoils [12].

The differential counting rate for a nucleus with mass  $m_N$  is

$$\frac{dR}{dE_d} = \frac{\rho_0}{m_N M} \int_{v_{\min}}^{\infty} v f(v) \frac{d\sigma_{BrN}}{dE_R}(v, E_R) dv, \quad (2)$$

where  $\rho_0$  is the local branon density,  $(d\sigma_{BrN}/dE_R)(v, E_R)$  is the differential cross-section for the Branon-nucleus elastic scattering, and  $f(v)$  is the Branon speed distribution in the detector frame normalized to unity.

The relative speed of a dark matter particle is of order  $100 \text{ km}^{-1} \text{ s}^{-1}$ , so the elastic scattering is nonrelativistic. Then, the recoil energy of the nucleon in terms of the scattering angle in the center of mass frame  $\theta^*$ , and the branon-nucleus reduced mass  $\mu_N = M m_N / (M + m_N)$ , is given by [12]

$$E_R = \frac{\mu_N^2 v^2 (1 - \cos\theta^*)}{m_N}. \quad (3)$$

The lower limit of the integration over the WIMP speed is given in terms of the minimum branon speed which can cause a recoil of energy  $E_R$  and is given by  $v_{\min} = (m_N E_R / 2\mu_N^2)^{1/2}$ . The upper limit is infinite; however, the local escape speed,  $v_{\text{esc}}$ , is the maximum speed in the Galactic rest frame for WIMPs which are gravitationally bound to the Milky Way. The standard value for this scape velocity is  $v_{\text{esc}} = 650 \text{ km s}^{-1}$  [12].

Integrating the differential event rate over all the possible recoil energies, it is possible to find the total event rate of branon collisions with matter per kilogram per day,  $R$ . The smallest recoil energy that the detector is capable of measuring is called threshold energy,  $E_T$ . In terms of this threshold energy,  $E_T$ , the total event rate  $R$  has the form [12]:

$$R = \int_{E_T}^{\infty} dE_R \frac{\rho_0}{m_N M} \int_{v_{\min}}^{\infty} v f(v) \frac{d\sigma_{BrN}}{dE_R}(v, E_R) dv. \quad (4)$$

The branon-nucleus differential cross section contains the particle physics inputs and depends on the branon-quark interaction given by (1). For a general DM candidate, its nucleus cross section is separated into a spin-independent (SI) scalar contribution and a spin-dependent (SD) one [12]:

$$\frac{d\sigma_N}{dE_R} = \frac{m_N}{2\mu_N^2 v^2} (\sigma_0^{\text{SI}} F_{\text{SI}}^2(E_R) + \sigma_0^{\text{SD}} F_{\text{SD}}^2(E_R)). \quad (5)$$

Here, the form factors  $F_{\text{SI}}(E_R)$  and  $F_{\text{SD}}(E_R)$  account for the coherence loss, which leads to a suppression in the event rate for heavy WIMPs on nucleons and includes the dependence on the momentum transfer  $q = \sqrt{2m_N E_R}$ .  $\sigma_0^{\text{SI}}$  and  $\sigma_0^{\text{SD}}$  are the spin-independent and spin-dependent cross

sections, respectively, at zero momentum transfer. These quantities still depend on nuclear structure through isospin content; that is, the number of protons vs neutrons [13].

In the branon case, the entire interaction is SI and can be written, in general, as [13]

$$\sigma_p^{\text{SI}} = \frac{[Zf_p + (A - Z)f_n]^2}{f_p^2} \frac{\mu_{\text{DM}n}^2}{\mu_{\text{DM}p}^2} \sigma_p^{\text{SI}}, \quad (6)$$

with  $A$  the atomic mass number,  $Z$  the charge of the nucleus,  $f_{p,n}$  the SI DM couplings to proton and neutron, respectively.  $\mu_{\text{DM}p}$  is the reduced DM-proton mass, and  $\sigma_p^{\text{SI}}$  the SI cross section for scattering of DM on a proton. In particular, branons do not violate isospin symmetry if we neglect the difference in mass of protons and neutrons. Therefore, within this approximation:  $f_p = f_n$ , and  $\mu \equiv \mu_{\text{Br}n} = \mu_{\text{Br}p}$ . Indeed, the branon-nucleon cross section  $\sigma_n$  can be written as [3]

$$\sigma_p^{\text{SI}} = \sigma_n = \frac{9M^2 m_n^2 \mu^2}{64\pi f^8}, \quad (7)$$

where  $m_n$  is the nucleon mass. Recently, direct search experiments have reported possible candidate events for DM. The annual modulation signature found either by the former DAMA/NAI and DAMA/LIBRA detectors localized in Gran Sasso National Laboratory points out to a light WIMP [14]. A similar conclusion can be obtained from the CoGeNT observations. This ultralow-noise germanium detector operated deep underground in Soudan Underground Laboratory has found some events consistent with a WIMP of mass 7 to 11 GeV [15]. However, these measurements are in clear tension with exclusion limits obtained by other experiments located in the same laboratories such as XENON100 (a liquid xenon detector at the Gran Sasso National Laboratory) [16], or CDMS II (a germanium and silicon detector at the Soudan Underground Laboratory) [17].

The CDMS Collaboration has reported two candidate events for DM that are consistent with heavier WIMPs and with the present constraints [17]. Indeed, the analysis was performed on data taken during four periods between July 2007 and September 2008, maximizing the expected sensitivity for a 60 GeV WIMP. Their spectrum-averaged equivalent exposure for a WIMP of this mass is 194.1 kg-days. Two events in the WIMP acceptance region were observed at recoil energies of 12.3 keV and 15.5 keV.

Neutrons with energies of several MeV can generate single-scatter nuclear recoils that are indistinguishable from possible DM interactions. Also, an approximation made during the ionization pulse reconstruction degrades the timing-cut rejection for a small fraction of surface events with ionization energy below 6 keV. Therefore, the probability to have observed two or more surface events in this exposure is estimated to 20%. Including the

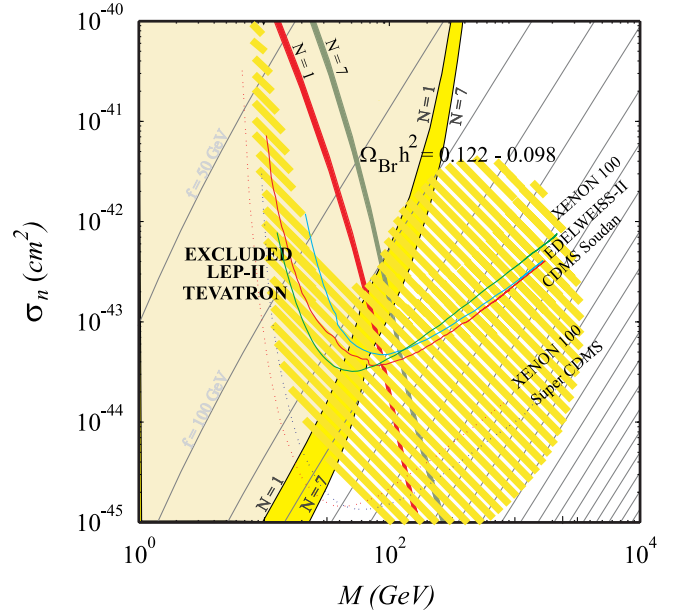


FIG. 1 (color online). Elastic branon-nucleon cross section  $\sigma_n$  in terms of the branon mass. The two thick lines correspond to the  $\Omega_{\text{Br}} h^2 = 0.122 - 0.098$  curve for cold branons with  $N = 1$  (left) and  $N = 7$  (right). The shaded areas on the left are the collider exclusion regions [6,8], also for  $N = 1, 7$ . The solid lines correspond to the current limits on the spin-independent cross section from direct detection experiments XENON 100 [16], EDELWEISS-II [27] and CDMS [17]. The striped area is favored by CDMS measurements [17] and the dotted lines are sensitivity prospects for XENON 100 and super CDMS.

neutron background, the candidate events have a probability 23% of not being due to a DM signal [17].

The results of the analysis for branon-nucleon cross section  $\sigma_n$  in terms of the branon mass and the limits of direct DM search experiments are shown in Fig. 1. For reference, lines of constant  $f$  with 50 GeV separation are shown. The area on the left of the  $\Omega_{\text{Br}} h^2 = 0.122 - 0.098$  curves is excluded by branon overproduction, but the area on the right is compatible with observations. These areas correspond to  $f \approx 120$  GeV and  $M \approx 40$  GeV, respectively. The dashed region is favored by the 2 CDMS II events at 12.3 keV and 15.5 keV at the 90% confidence level.

#### IV. COLLIDERS SEARCHES AT THE LHC

If the new physics able to explain the DM puzzle is related to the electroweak scale, it may be accessible at the LHC and in the new generation of collider experiments [7,8].

The most important process for branon production in a proton-proton collider, such as the LHC, is given by the gluon fusion giving a gluon and a branon pair; as well as a quark-gluon interaction giving a quark and a branon pair. In these cases, the expected experimental signal is one

monojet  $J$  and missing energy and momentum which can easily be identified. An additional interesting process is the quark-antiquark annihilation giving a photon and a branon pair. For this process, the signature is one single photon and missing energy and momentum. All the branons are assumed to be degenerated with a common mass  $M$  and the quarks are considered massless. Top quark production has been neglected due to its large mass.

The cross section of the subprocess  $gg \rightarrow g\pi\pi$  is given by [8]

$$\begin{aligned} \frac{d\sigma(gg \rightarrow g\pi\pi)}{dk^2 dt} &= \frac{\alpha_s N (k^2 - 4M^2)^2}{40960 f^8 \pi^2 \hat{s}^3 tu} \\ &\times \sqrt{1 - \frac{4M^2}{k^2} (\hat{s}^4 + t^4 + u^4 - k^8 + 6k^4(\hat{s}^2 + t^2 + u^2) - 4k^2(\hat{s}^3 + t^3 + u^3))}, \end{aligned} \quad (8)$$

where  $\hat{s} \equiv (p_1 + p_2)^2$ ,  $t \equiv (p_1 - q)^2$ ,  $u \equiv (p_2 - q)^2$ , and  $k^2 \equiv (k_1 + k_2)^2$ .  $p_1$  and  $p_2$  are the initial gluon four-momenta,  $q$  the final gluon four-momentum, and  $k = k_1 + k_2$  the total branon four-momentum. Therefore, the contribution to the total cross section for the  $pp \rightarrow g\pi\pi$  reaction coming from this subprocess is given by

$$\begin{aligned} \sigma_{gg}(pp \rightarrow g\pi\pi) &= \int_{x_{\min}}^1 dx \int_{y_{\min}}^1 dy g(y; \hat{s}) g(x; \hat{s}) \\ &\times \int_{k_{\min}^2}^{k_{\max}^2} dk^2 \int_{t_{\min}}^{t_{\max}} dt \frac{d\sigma(gg \rightarrow g\pi\pi)}{dk^2 dt}. \end{aligned} \quad (9)$$

Here,  $g(x; s)$  is the gluon distribution function of the proton,  $x$  and  $y$  are the fractions of the protons energy carried by the initial gluons. The different limits of the integrals can be written in terms of the cuts used to define the total cross section. For example, in order to be able to detect clearly the monojet, a minimal value for its transverse energy  $E_T$  and a pseudorapidity range given by  $\eta_{\min}$  and  $\eta_{\max}$  must be imposed. Then, the limits  $k_{\min}^2 = 4M^2$ ,  $k_{\max}^2 = \hat{s}(1 - 2E_T/\sqrt{\hat{s}})$  and  $t_{\min(\max)} = -(\hat{s} - k^2) \times [1 + \tanh(\eta_{\min(\max)})]/2$  are obtained. Also, we have  $x_{\min} = s_{\min}/s$  and  $y_{\min} = x_{\min}/x$ , where  $s$  is the total center of mass energy squared of the process and

$$s_{\min} = 2E_T^2 + 4M^2 + 2E_T \sqrt{E_T^2 + 4M^2}. \quad (10)$$

For the  $qg \rightarrow q\pi\pi$  subprocess, the cross section is given by [8]

$$\begin{aligned} \frac{d\sigma(qg \rightarrow q\pi\pi)}{dk^2 dt} &= \frac{\alpha_s N (k^2 - 4M^2)^2}{2 \cdot 184320 f^8 \pi^2 \hat{s}^3 tu} \\ &\times \sqrt{1 - \frac{4M^2}{k^2} (uk^2 + 4t\hat{s})(2uk^2 + t^2 + \hat{s}^2)}, \end{aligned} \quad (11)$$

with  $p_1$  and  $p_2$  being the quark and the gluon four-momenta, respectively,  $q$  the final state quark four-momentum, and  $k_1$  and  $k_2$  the branon four-momenta. The Mandelstam variables are defined as in previous cases.

The total cross section for the reaction  $pp \rightarrow q\pi\pi$  is then

$$\begin{aligned} \sigma(pp \rightarrow q\pi\pi) &= \int_{x_{\min}}^1 dx \int_{y_{\min}}^1 dy \sum_q g(y; \hat{s}) q_p(x; \hat{s}) \\ &\times \int_{k_{\min}^2}^{k_{\max}^2} dk^2 \int_{t_{\min}}^{t_{\max}} dt \frac{d\sigma(qg \rightarrow q\pi\pi)}{dk^2 dt}. \end{aligned} \quad (12)$$

In this equation,  $x$  and  $y$  are the fractions of the energy of the two protons carried by the subprocess quark and gluon. The different limits of the integrals can be written as in the previous case in terms of the minimal transverse energy of the quark (monojet)  $E_T$ .

Considering all the above equations, it is possible to compute the total cross section  $\sigma(pp \rightarrow J\pi\pi)$  in terms of the cut in the jet transverse energy  $E_T$ .

On the other hand, to analyze the single-photon channel, we need the cross section of the subprocess  $q\bar{q} \rightarrow \gamma\pi\pi$ , that was computed in [8]:

$$\begin{aligned} \frac{d\sigma(q\bar{q} \rightarrow \gamma\pi\pi)}{dk^2 dt} &= \frac{Q_q^2 \alpha N (k^2 - 4M^2)^2}{184320 f^8 \pi^2 \hat{s}^3 tu} \\ &\times \sqrt{1 - \frac{4M^2}{k^2} (\hat{s}k^2 + 4tu)(2\hat{s}k^2 + t^2 + u^2)}. \end{aligned} \quad (13)$$

And this is the only leading contribution:

$$\begin{aligned} \sigma(pp \rightarrow \gamma\pi\pi) &= \int_{x_{\min}}^1 dx \int_{y_{\min}}^1 dy \sum_q \bar{q}_p(y; \hat{s}) q_p(x; \hat{s}) \\ &\times \int_{k_{\min}^2}^{k_{\max}^2} dk^2 \int_{t_{\min}}^{t_{\max}} dt \frac{d\sigma(q\bar{q} \rightarrow \gamma\pi\pi)}{dk^2 dt}. \end{aligned} \quad (14)$$

By using all these cross sections, it is possible to compute the expected number of events in these channels produced at the LHC in terms of the brane tension scale  $f$ , the branon mass  $M$ , and the number of branons  $N$ . The main source of uncertainty is coming from the parton distribution function that we have taken from [18].

Previous constraints on the branon model parameter for tree-level processes from other colliders are summarized in Table I [6–8]. In this Table, the present restrictions coming

TABLE I. Limits from direct branon searches at colliders (results at the 95% c.l.). Upper indices 1, 2 denote monojet and single-photon channels, respectively. Current data [19–21] and prospects for the LHC are compared with present constraints from LEP [7], HERA and Tevatron [8].  $\sqrt{s}$  is the center of mass energy of the total process;  $\mathcal{L}$  is the total integrated luminosity;  $f_0$  is the bound on the brane tension scale for one massless branon ( $N = 1$ ); and  $M_0$  is the limit on the branon mass for small tension  $f \rightarrow 0$ . It is important to note that the effective approach taken in this analysis that allows to write Lagrangian (1) is not valid for energy scales  $\Lambda \gtrsim 4\pi^{1/2}fN^{-1/4}$  [5]. Therefore, the  $M_0$  value cannot be trusted. In any case, we are providing this number since it is the simplest way to characterize the sensitivity of the analysis for heavy branons.

Experiment	$\sqrt{s}$ (TeV)	$\mathcal{L}$ (pb $^{-1}$ )	$f_0$ (GeV)	$M_0$ (GeV)
HERA <sup>1</sup>	0.3	110	16	152
Tevatron-II <sup>1</sup>	2.0	10 <sup>3</sup>	256	902
Tevatron-II <sup>2</sup>	2.0	10 <sup>3</sup>	240	952
LEP-II <sup>2</sup>	0.2	600	180	103
LHC <sup>1</sup>	7	3.4 × 10 <sup>-4</sup>	189	3240
LHC <sup>1</sup>	7	11.7 × 10 <sup>-3</sup>	236	3240
LHC <sup>2</sup>	7	1.21 × 10 <sup>-3</sup>	152	3390
LHC <sup>1</sup>	14	10 <sup>5</sup>	1075	6481
LHC <sup>2</sup>	14	10 <sup>5</sup>	797	6781

from HERA, Tevatron and LEP-II are compared with the present LHC bounds running at a center of mass energy (c.m.e.) of 7 TeV and the prospects for the LHC running at 14 TeV c.m.e. with full luminosity. For the single-photon channel, ATLAS has published two different analysis with a total integrated luminosity of 0.68 nb $^{-1}$  and 0.53 nb $^{-1}$  [19]. The results are not well understood within present hadron interaction models, but we can deduce the constraints showed in Table I by assuming a conservative approach. In any case, it is much more interesting than the analysis presented by CMS about jet and missing transverse energy, which is the most constraining one for branon phenomenology due to its high luminosity: 11.7 nb $^{-1}$  [20]. In order to complete the analysis, we have included in Table I, the analogous study by ATLAS which is not competitive due to the low luminosity of 0.34 nb $^{-1}$  used in the analysis [21].

In addition, it has been shown that branon loops introduce new couplings among SM particles that can be described by an effective Lagrangian. The most relevant terms of this effective Lagrangian are [5]:

$$\mathcal{L}_{\text{SM}}^{(1)} \simeq \frac{N\Lambda^4}{192(4\pi)^2 f^8} \{2T_{\mu\nu}T^{\mu\nu} + T_{\mu}^{\mu}T_{\nu}^{\nu}\}. \quad (15)$$

The  $\Lambda$  parameter appears when dealing with branon radiative corrections since the Lagrangian (1) is not renormalizable. This parameter is the cutoff which limits the validity of the effective description of branon and SM dynamics. A one-loop calculation with the new effective four-fermion vertices coming from (16) is equivalent to a two-loop

TABLE II. Limits from virtual branon searches at colliders (results at the 95% c.l.). The indices  $a, b, c$  denote the two-photon,  $e^+e^-$ , and  $e^+p$  ( $e^-p$ ) channels, respectively [5]. Present constraints from HERA, LEP, and Tevatron are compared with the LHC prospects. The first two columns are the same as in Table I, and the third one corresponds to the lower bound on  $f^2/(N^{1/4}\Lambda)$ . In this case, current LHC constraints are not competitive.

Experiment	$\sqrt{s}$ (TeV)	$\mathcal{L}$ (pb $^{-1}$ )	$f^2/(N^{1/4}\Lambda)$ (GeV)
HERA <sup>c</sup>	0.3	117	52
Tevatron <sup>a,b</sup>	1.8	127	69
LEP <sup>a</sup>	0.2	700	59
LEP <sup>b</sup>	0.2	700	75
LHC <sup>b</sup>	14	10 <sup>5</sup>	383

computation with the Lagrangian in (1), and it also allows to obtain the contribution of branons to the anomalous magnetic moment of the muon [5]:

$$\delta a_{\mu} \simeq \frac{5m_{\mu}^2}{114(4\pi)^4} \frac{N\Lambda^6}{f^8}, \quad (16)$$

where  $N$  is the number of branon species.

The most relevant branon loops that could have compatible effects with SM phenomenology could be the

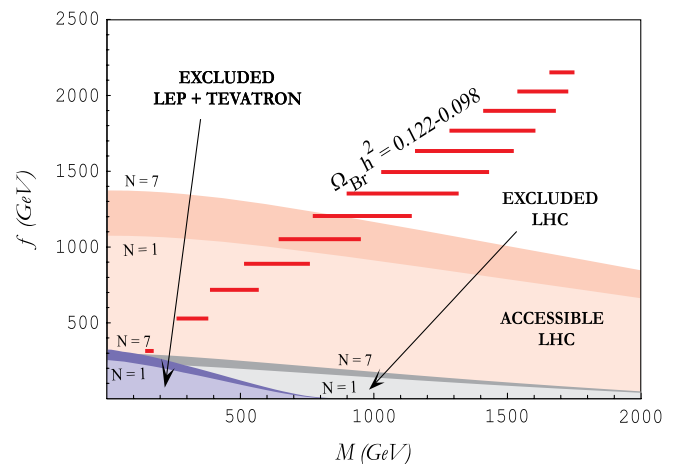


FIG. 2 (color online). The shaded area shows the parameter space of the branon model with a thermal relic in the range:  $\Omega_{\text{Br}}h^2 = 0.122 - 0.098$ , a contribution to the muon anomalous magnetic moment:  $a_{\mu} = (29 \pm 18) \times 10^{-10}$  and favored by the CDMS data. The lower area is excluded by single-photon processes at LEP together with monojet signals at Tevatron [6,8]. Jet and missing energy analyses performed with LHC data are the most constraining for heavy branons (intermediate area). Prospects for the sensitivity at the LHC for real branon production are plotted also for the monojet analysis for a total integral luminosity of  $\mathcal{L} = 10^5$  and total energy in the center of mass of the collision of  $\sqrt{s} = 14$  TeV. The explicit dependence on the number of branons  $N$  is presented, since all these regions are plotted for the extreme values  $N = 1$  and  $N = 7$ .

four-fermion interactions or the fermion pair annihilation into two gauge bosons [5]. Bounds on the parameter combination  $f^2/(\Lambda N^{1/4})$  can be established by considering current data. Present results are shown in Table II, where it is also possible to find the prospects for LHC [5]. However, in contrast to branon direct production, current measurements by CMS or ATLAS detectors are not able to improve the limits obtained with data coming from HERA [22], Tevatron [23] and LEP [24].

The preferred parameter region for branon physics is given by [5]

$$6.0 \text{ GeV} \gtrsim \frac{f^4}{N^{1/2} \Lambda^3} \gtrsim 2.2 \text{ GeV} \quad (95\% \text{ c.l.}) \quad (17)$$

As a result of this relation and the limits shown in Table II, the first branon signals at colliders would be associated to radiative corrections [5].

## V. CONCLUSIONS

Brane fluctuations are DM candidates in brane world models with low tension. We have studied the current situation of branons in relation with direct dark matter detection experiments and recent LHC measurements. As shown in Fig. 2, the results show that, in a certain range of the parameters for the brane tension  $f$  and branon mass  $M$ , the relic abundance could explain the missing mass problem and that such parameter regions would be compatible with DM candidate events currently observed by direct

search experiments, if these events are due to branon-nucleus coherent interactions.

In spite of the current low luminosity of the LHC, present constraints from ATLAS and CMS are the most constraining for heavy branons, improving previous analyses performed with LEP-II and TEVATRON data. In any case, for light branons, these analyses are still the most important. The same situation is found for SM processes mediated by virtual branons, where current LHC measurements are not competitive yet.

In addition, there are other signatures which can prove or disprove the model. It could be possible to detect branons in DM indirect search experiments [25]. Two branons may annihilate into ordinary SM matter. Their annihilation in places like the Galactic halo, the Sun, the Earth, etc., could produce cosmic rays to be discriminated through distinctive signatures from the background. After annihilation, a cascade process would occur and particles such as neutrinos, gamma rays, positrons, or antimatter may be detectable through different experiments such as Atmospheric Cerenkov Telescopes, Neutrino Telescopes, or Satellite Detectors. Work is in progress in this direction [26].

## ACKNOWLEDGMENTS

This work is supported in part by DOE Grant Nos. FG02-94ER40823, FPA 2005-02327 project (DGICYT, Spain), CAM/UCM 910309 project, MICINN Consolider-Ingenio MULTIDARK CSD2009-00064, CONACYT (Mexico), and SNI (Mexico).

- 
- [1] L. Covi, J.E. Kim, and L. Roszkowski, *Phys. Rev. Lett.* **82**, 4180 (1999); J.L. Feng, A. Rajaraman, and F. Takayama, *Phys. Rev. D* **68**, 085018 (2003); *Int. J. Mod. Phys. D* **13**, 2355 (2004); J.A.R. Cembranos, J.L. Feng, A. Rajaraman, and F. Takayama, *Phys. Rev. Lett.* **95**, 181301 (2005); J.A.R. Cembranos, J.L. Feng, and L.E. Strigari, *Phys. Rev. D* **75**, 036004 (2007); [arXiv:0708.0247](#); [arXiv:0708.0239](#); J.A.R. Cembranos, J.H. Montes de Oca, and L. Prado, *J. Phys. Conf. Ser.* **315**, 012012 (2011); J.A.R. Cembranos, *Phys. Rev. Lett.* **102**, 141301 (2009); *AIP Conf. Proc.* **1182**, 288 (2009); *Phys. Rev. D* **73**, 064029 (2006); , in *AIP Conf. Proc.* 1343, 604 (AIP, New York, 2011). J.A.R. Cembranos, K.A. Olive, M. Peloso, and J.P. Uzan, *J. Cosmol. Astropart. Phys.* **07** (2009) 025; T. Biswas, J.A.R. Cembranos, and J.I. Kapusta, *Phys. Rev. Lett.* **104**, 021601 (2010); *J. High Energy Phys.* **10** (2010) 048; *Phys. Rev. D* **82**, 085028 (2010).
- [2] H. Goldberg, *Phys. Rev. Lett.* **50**, 1419 (1983); J.R. Ellis *et al.*, *Nucl. Phys.* **B238**, 453 (1984); K. Griest and M. Kamionkowski, *Phys. Rep.* **333–334**, 167 (2000).
- [3] J.A.R. Cembranos, A. Dobado, and A.L. Maroto, *Phys. Rev. Lett.* **90**, 241301 (2003); *Phys. Rev. D* **68**, 103505 (2003).
- [4] M. Bando *et al.*, *Phys. Rev. Lett.* **83**, 3601 (1999).
- [5] J.A.R. Cembranos, A. Dobado, and A.L. Maroto, *Phys. Rev. D* **73**, 035008 (2006); *Phys. Rev. D* **73**, 057303 (2006).
- [6] A. Dobado and A.L. Maroto, *Nucl. Phys.* **B592**, 203 (2001); J. Alcaraz *et al.*, *Phys. Rev. D* **67**, 075010 (2003); J.A.R. Cembranos, A. Dobado, and A.L. Maroto, *AIP Conf. Proc.* **670**, 235 (2003); [arXiv:hep-ph/0402142](#); [arXiv:hep-ph/0406076](#); [arXiv:hep-ph/0411076](#); [arXiv:astro-ph/0411262](#); *Int. J. Mod. Phys. D* **13**, 2275 (2004); [arXiv:astro-ph/0503622](#); [arXiv:astro-ph/0512569](#); [arXiv:astro-ph/0611911](#); A.L. Maroto, *Phys. Rev. D* **69**, 043509 (2004); *Phys. Rev. D* **69**, 101304 (2004); J.A.R. Cembranos *et al.*, [arXiv:0708.0235](#); *J. Cosmol. Astropart. Phys.* **0810** (2008) 039.
- [7] P. Achard *et al.*, *Phys. Lett. B* **597**, 145 (2004); S. Heinemeyer *et al.*, [arXiv:hep-ph/0511332](#); J.A.R. Cembranos, A. Rajaraman, and F. Takayama, [arXiv:hep-ph/0512020](#); *Europhys. Lett.* **82**, 21001 (2008); J.A.R.

- Cembranos, A. Dobado, and A. L. Maroto, [arXiv:hep-ph/0107155](https://arxiv.org/abs/hep-ph/0107155); *Phys. Rev. D* **65**, 026005 (2001); [arXiv:hep-ph/0307015](https://arxiv.org/abs/hep-ph/0307015); *J. Phys. A* **40**, 6631 (2007); [arXiv:hep-ph/0512302](https://arxiv.org/abs/hep-ph/0512302); A. Juste *et al.*, [arXiv:hep-ph/0601112](https://arxiv.org/abs/hep-ph/0601112); J. A. R. Cembranos *et al.*, [arXiv:hep-ph/0603067](https://arxiv.org/abs/hep-ph/0603067); *AIP Conf. Proc.* **903**, 591 (2007); ILC Collaboration, [arXiv:0709.1893](https://arxiv.org/abs/0709.1893); ILC Collaboration, [arXiv:0712.1950](https://arxiv.org/abs/0712.1950); ILC Collaboration, [arXiv:0712.2356](https://arxiv.org/abs/0712.2356); T. E. Clark *et al.*, *Phys. Rev. D* **78**, 115004 (2008).
- [8] J. A. R. Cembranos, A. Dobado, and A. L. Maroto, *Phys. Rev. D* **70**, 096001 (2004).
- [9] S. S. Gubser, I. R. Klebanov, and A. W. Peet, *Phys. Rev. D* **54**, 3915 (1996); I. R. Klebanov, *Nucl. Phys.* **B496**, 231 (1997).
- [10] R. Sundrum, *Phys. Rev. D* **59**, 085009 (1999); T. Kugo and K. Yoshioka, *Nucl. Phys.* **B594**, 301 (2001); P. Creminelli and A. Strumia, *Nucl. Phys.* **B596**, 125 (2001); S. C. Park and H. S. Song, *Phys. Lett. B* **523**, 161 (2001).
- [11] PDG web page: <http://pdg.lbl.gov/2010/reviews/rpp2010-rev-dark-matter.pdf>.
- [12] D. G. Cerdeño and A. M. Green, *Particle Dark Matter: Observations, Models and Searches*, edited by G. Bertone (Cambridge University Press, Cambridge, 2010), p. 347–369.
- [13] J. Kopp, T. Schwetz, and J. Zupan, *J. Cosmol. Astropart. Phys.* 014, 1002 (2010).
- [14] R. Bernabei *et al.* (DAMA collaboration), *Eur. Phys. J. C* **67**, 39 (2010).
- [15] C. E. Aalseth *et al.* (CoGeNT collaboration), *Phys. Rev. Lett.* **106**, 131301 (2011).
- [16] E. Aprile *et al.* (XENON100 Collaboration), [arXiv:1104.2549v2](https://arxiv.org/abs/1104.2549v2).
- [17] Z. Ahmed *et al.* (CDMS Collaboration), *Science* **327**, 1619 (2010).
- [18] A. D. Martin *et al.*, *Eur. Phys. J. C* **4**, 463 (1998); H. L. Lai *et al.*, *Eur. Phys. J. C* **12**, 375 (2000); <http://durpdg.dur.ac.uk>.
- [19] O. Adriani *et al.*, *Phys. Lett. B* **703**, 128 (2011).
- [20] J. Weng (CMS collaboration), *Proc. Sci.*, ICHEP (2010) 028.
- [21] A. Schwartzman, *Proc. Sci.*, ICHEP (2010) 023.
- [22] C. Adloff *et al.*, *Phys. Lett. B* **568**, 35 (2003).
- [23] B. Abbott *et al.*, *Phys. Rev. Lett.* **86**, 1156 (2001).
- [24] D. Abbaneo *et al.*, [arXiv:hep-ex/0412015](https://arxiv.org/abs/hep-ex/0412015).
- [25] J. A. R. Cembranos and L. E. Strigari, *Phys. Rev. D* **77**, 123519 (2008); J. A. R. Cembranos, J. L. Feng, and L. E. Strigari, *Phys. Rev. Lett.* **99**, 191301 (2007); J. A. R. Cembranos, *et al.*, *Phys. Rev. D* **83**, 083507 (2011); , *AIP Conf. Proc.* 1343, 595 (AIP, New York, (2011); [arXiv:1012.4473](https://arxiv.org/abs/1012.4473).
- [26] J. A. R. Cembranos, A. de la Cruz-Dombriz, V. Gammaldi, and A. L. Maroto (unpublished).
- [27] E. Armengaud *et al.* (EDELWEISS Collaboration), *Phys. Lett. B* **702**, 329 (2011).
- [28] J. L. Hewett, *Phys. Rev. Lett.* **82**, 4765 (1999).